

NWRI CONTRIBUTION 85-14

Ng (18)

Marsalek (66)

Study 83-334

ENERGY LOSSES AT JUNCTION MANHOLES

WITH A LATERAL

by

Howard Ng and Jiri Marsalek

Environmental Hydraulics Section
Hydraulics Division
National Water Research Institute
Canada Centre for Inland Waters
Burlington, Ontario, Canada L7R 4A6

November 1984

ABSTRACT

Head losses at sewer junctions of a main pipe with a lateral were studied for various junction geometries and pressurized flow characteristics. The junction parameters studied included the manhole base shape, the size and angle of entry of the lateral pipe, and various benchings installed in the junction manhole. The most important flow variable was the relative lateral inflow ($=Q_{\text{lateral}}/Q_{\text{outlet}}$). The junction head losses were affected most by the lateral pipe size and the relative lateral inflow.

RESUME

On étudié les pertes d'énergie aux raccordements entre un égout principal et un égout latéral en fonction de la forme du raccordement et des régimes d'écoulement forcé. Pour ce qui est du regard proprement dit, voici les paramètres que nous avons retenus: forme de la base de l'ouvrage, divers types de banquettes de circulation dont il est muni, ainsi que diamètre et angle d'arrivée de l'égout latéral. Quant au régime d'écoulement, la variable la plus importante a été le débit relatif de l'égout latéral (correspondant au rapport $Q_{\text{latéral}}/Q_{\text{sortie}}$). On a conclu que les chutes d'énergie de l'écoulement dans les raccordements tiennent surtout au diamètre de l'égout latéral et au débit relatif de celui-ci.

TABLE OF CONTENTS

	<u>PAGE</u>
ABSTRACT	i
1.0 INTRODUCTION	1
2.0 EXPERIMENTAL APPARATUS AND PROCEDURES	1
2.1 Experimental Apparatus	1
2.2 Experimental Procedures	2
3.0 DATA ANALYSIS	3
3.1 Energy Grade Lines for Test Pipes	3
3.2 Calculation of Energy Losses at Junctions	3
4.0 EXPERIMENTAL RESULTS	5
4.1 Data Presentation	6
4.2 Combined Head Loss Coefficients for Various Junction Configurations	7
5.0 DISCUSSION OF RESULTS	8
6.0 SUMMARY AND CONCLUSIONS	10
7.0 REFERENCES	12

LIST OF TABLES

- Table 1. Coefficients of Quadratic Regression Polynomials
- Table 2. Combined Head Loss Coefficients for Various Lateral Inflows
- Table 3. Comparison of Head Loss Coefficients from Various Sources

LIST OF FIGURES

- Figure 1. General Layout of Experimental Apparatus
- Figure 2. Junction Box with a Lateral Pipe Inlet Assembly
- Figure 3. Junction Manhole with Benchings Tested
- Figure 4. Notation Sketch
- Figure 5. Head Loss Coefficient vs the Relative Lateral Inflow

1.0 INTRODUCTION

Head losses at sewer pipe junctions have been investigated in the Hydraulics Laboratory of the Hydraulics Division of the National Water Research Institute during the last several years. While the first phase of these investigations dealt with head losses at straight-flow-through junctions (4) the phase described in this report deals with head losses at junctions of a main pipe with a single lateral.

The main objectives of these studies were to evaluate junction head losses caused by a lateral inflow at various angles, and to investigate flow guidance devices for reduction of such losses. The basic junction structure studied was a square-base manhole with a main pipe and a lateral pipe entering the junction at three different angles - 45°, 60° and 90°. A round-base manhole was investigated only for a 90° lateral. In all experiments, the flow in the pipe was pressurized.

2.0 EXPERIMENTAL APPARATUS AND PROCEDURES

2.1 Experimental Apparatus

A general layout of the experimental apparatus is shown in Figure 1. The apparatus consists of two water supply tanks, the main pipe, the lateral pipe, the junction box, and a measuring weir box. The junction assembly is shown in Figure 2.

Both the main and lateral pipes were clear acrylic pipes. The internal diameter of the main pipe was 152 mm throughout the installation. Four lateral pipe sizes were used, with internal radii of 76, 102, 127 and 152 mm, respectively. Both main and lateral pipe branches consisted of a number of sections which were typically 1.82 m long. The individual sections were connected by means of rubber sleeves and metal band clamps. The main pipe branches upstream and downstream of the junction were 16.47 m and 9.15 m long, respectively. The lateral pipe

was 3.80 m long. The hydraulic resistance of the main pipe was characterized in the earlier tests (4) by the roughness factor of $K = 0.034$ mm (after the Colebrook-White equation).

The acrylic pipes were supported by a TV antenna beam resting on 13 scissor jacks. The pipe slope was changed manually by gradually adjusting individual jacks. In all runs, the pipes were set at slope of 0.01. Piezometer openings were formed by drilling 3 mm diameter holes in pipe inverts at 0.6 m intervals. A total of 47 piezometer openings were drilled; 20 openings in the upstream pipe, 16 openings in the downstream pipe, and 11 openings in the lateral pipe. The lateral pipe piezometers were spaced at 0.305 m intervals. The piezometer openings were connected to a manometer board by Tygon tubing. On the board, piezometer heads were read with an accuracy of ± 0.5 mm.

The dimensions of the square-base junction manhole are shown in Fig. 2. A round-base manhole was obtained by installing a cylindrical insert in the basic manhole. In all tests, the ends of the test pipes attached to the junction manhole had square edges.

Sketches of all junction geometries tested are shown in Fig. 3. The main variables included the manhole base shape, the lateral pipe size and angle, and the benching (mould and deflectors) inside the junction.

2.2 Experimental Procedures

When studying head losses in individual junction configurations, the main experimental variable was the relative discharge defined as $\psi_{13} = Q_3/Q_1$, where Q_3 is the lateral discharge, and Q_1 is the outlet discharge ($Q_1 = Q_3 + Q_2$, where Q_2 is the main pipe discharge). To obtain various relative discharges, a constant main pipe discharge was established first and then the lateral discharge was varied over a fairly wide range. For each setting of the relative discharge, the flow rates through the lateral and outlet pipes were measured by taking

measuring weir readings, and all the piezometer readings were photographically recorded.

Using the observed piezometric readings and the velocity heads calculated from observed discharges, energy grade lines were determined for all pipe reaches and projected to the junction. The drops in the grade line, at the junction, for the main and lateral pipes were then taken as junction head losses for the main and lateral pipes, respectively.

Altogether 40 junction configurations were tested using the experimental procedures outlined above. Each junction configuration tested is referred to by a test series number in the following sections.

It should be emphasized that, in order to simplify the testing procedures, only the discharge through the lateral pipe was varied.

3.0 DATA ANALYSIS

3.1 Energy Grade Lines for Test Pipes

The first step in the processing of experimental data was to plot energy heads for individual piezometers. Using the least-squares method, straight lines were fitted through the plotted points in order to obtain energy grade lines for all three test pipes. Such a fitting procedure helped to reduce effects of random errors in individual piezometer readings. A typical plot of least-squares fitted energy grade lines is shown in Figure 4.

3.2 Calculation of Energy Losses at Junctions

To determine the energy losses across the junction, the upstream and downstream grade lines, for both the main and lateral pipes, were projected to the centreline of the junction and the difference between the upstream and downstream grade lines, measured at the junction centreline, was taken as the junction loss. The same

procedure has been used earlier by many other researchers (2, 4, 5, 7 and 9).

Following the customary procedures, the measured energy head losses were expressed as the head loss coefficient, one for the main pipe,

$$K_{12} = \frac{\Delta E_{12}}{\frac{\bar{v}_1^2}{2g}} \quad (1)$$

and the other one for the lateral pipe

$$K_{13} = \frac{\Delta E_{13}}{\frac{\bar{v}_1^2}{2g}} \quad (2)$$

where K_{12} and K_{13} are the head loss coefficients for the main and lateral pipes, respectively,

ΔE_{12} and ΔE_{13} are the junction energy head losses for the main and lateral pipe, respectively (see Fig. 4),

\bar{v}_1 is the mean velocity in the outlet pipe, and
 g is the acceleration due to the gravity.

Furthermore, in order to compare the effect of different junction configurations on the overall energy loss, a combined energy head loss coefficient was calculated as follows (2, 3):

$$K_c = K_{12} \psi_{12} + K_{13} \psi_{13} \quad (3)$$

where K_c is the combined energy loss coefficient at the junction, K_{12} and K_{13} were defined before, and

$$\psi_{12} = Q_2/Q_1 \text{ and } \psi_{13} = Q_3/Q_1$$

where Q_2 is the main pipe discharge, Q_3 is the lateral discharge, and Q_1 is the outlet discharge. Note that $\psi_{12} + \psi_{13} = 1.0$.

4.0 EXPERIMENTAL RESULTS

Head loss coefficients observed in the junction model were plotted against the flow ratios in Figure 5. There are altogether 40 graphs shown in Figure 5, representing 40 different junction configurations tested. The graphs numbers correspond to the earlier listed test numbers from 1 to 40. Each graph indicates the angle between the main and lateral pipes (lateral angle), lateral pipe diameter (ϕ), and the junction benching geometry (M). The main and outlet pipes sizes were identical in diameter (152 mm).

The head loss coefficients, K_{12} and K_{13} , which are plotted against the relative discharges, ψ_{12} and ψ_{13} , in Fig. 5, typically varied from -0.5 to 12.0. This range of values indicates that head loss coefficients can be either positive or negative depending on whether energy is transferred to or from the lateral flow. Thus negative values of both head loss coefficients are plausible under certain circumstances and have been reported earlier by several investigators (3, 6, and 8).

The negative values of the lateral head loss coefficient K_{13} have been found for both 45° and 90° laterals for very small values of ψ_{13} (say $\psi_{13} < 0.3$), when almost all flow is passing through the main pipe. Under such circumstances, the water in the lateral appears to be drawn out by the main flow in a manner resembling ejector action. For these small lateral flows, the pressure in the lateral outlet is equal to that at the junction and the flow velocity is very small. As the water from the lateral is drawn into the main stream, an apparent energy gain takes place when basing the downstream pipe energy on the mean flow velocity in this pipe. However, this energy gain is only apparent, because the water flowing from the lateral must enter into the main flow region in which the velocity is below the mean value. In

connection with this discussion, two other points should be made - negative head losses (apparent energy gains) are neglected in practical design, and the combined head loss coefficient described by Eq. 3 is always positive.

The above explanation of apparent negative head losses also applies to the main pipe head loss coefficient K_{12} for the tested lateral angles 45° and 60° , and low values of ψ_{12} (i.e., almost all flow passing through the lateral).

Besides the physically plausible negative head loss coefficients, some extrapolations of observed K_{12} 's also yielded small negative values for the lateral angle of 90° . Such negative values are not physically plausible and these extrapolations were omitted from the final plots shown in Fig. 5.

4.1 Data Presentation

In each experimental series, the head loss coefficients K_{12} and K_{13} were determined for about 5 to 8 different values of the relative discharges ψ_{12} and ψ_{13} . Consequently, it was desirable to approximate such data by regression lines which could be used for data interpolation and extrapolation. After testing several regression models, a second degree polynomial model was found satisfactory for all 40 test series. This model was defined as follows:

$$K_{12} = a + b \psi_{12} + c \psi_{12}^2 \quad (4)$$

$$K_{13} = d + e \psi_{13} + f \psi_{13}^2 \quad (5)$$

where a , b , c , d , e and f are fitted coefficients.

Equations (4) and (5) were derived with an assumption that the head loss coefficients do not vary with the Reynolds number which can be defined as $Re = v D/\nu$, where v is the mean combined flow velocity, D is the pipe diameter, and ν is the kinematic viscosity. Thus for the experimental conditions studied, the head loss

coefficients are not affected by the combined discharge magnitude, but only by the division of discharges between the main and branch pipes. This assumption was based on extensive experimental evidence (5, 6 and 8) which indicated that, for Reynolds numbers greater than a certain threshold value, the head loss coefficients are independent of the Reynolds number. Although this threshold value was reported as low as 5×10^3 , the more commonly accepted value is 10^5 (6).

All the experiments reported here were performed in the range of Reynolds numbers from 1.8×10^5 to 3.4×10^5 . The head loss coefficients derived from these experiments are directly applicable to sewer design which can be characterized by Reynolds numbers greater than 1.4×10^5 . This minimum Re value follows from standard design practices which specify the minimum pipe diameter ($D = 0.305$ m) and the minimum flow velocity ($v = 0.61$ m/s), and from assumed kinematic viscosity of 1.3×10^{-6} m²/s. In applications to laminar and transitional flow, which are outside of the scope of this report, the head loss coefficients are affected by the Reynolds number (1) and equations (4) and (5) are no longer applicable.

Using Eqs. (4) and (5) and the regression coefficients given in Table 2, the head loss coefficients K_{12} and K_{13} can be calculated for arbitrary relative discharges ψ_{12} and ψ_{13} .

4.2 Combined Head Loss Coefficient for Various Junction Configurations

In order to compare the effect of different junction configurations on the overall energy loss, a combined head loss coefficient was calculated for each test series using Equation (3) and the data from Table 1. The results of such calculations are shown in Table 2.

The calculated K_C values shown in Table 2 range from a low of -0.533 (test series 36) to a high value of 17.82 (test series 15). Because of such large variations, the comparisons of results for

various junction configurations are difficult. To facilitate such comparisons, the mean \bar{K}_C , the standard deviation about the mean, and the coefficient of variation $c_v = \sigma/\bar{K}_C$ were calculated for all test series and also presented in Table 2.

5.0 DISCUSSION OF RESULTS

The discussion which follows is based on the results of extensive tests of head losses at sewer junctions with a lateral. Forty different junction configurations with various lateral sizes and angles, junction benchings (moulds), and manhole bases were tested for pressurized flow conditions. Considering the need to test each configuration for a range of flow divisions, more than 250 experiments had to be conducted.

The head loss coefficients K_{12} and K_{13} shown in Fig. 5 varied with the relative discharges ψ_{12} and ψ_{13} . Such variations were found nonlinear and for practical purposes could be approximated by polynomials of the second degree. The fitted coefficients of such polynomials were given in Table 2 and could be used to calculate head coefficients for the relative discharges ψ_{12} and ψ_{13} varying from 0 to 1.0. Such calculated head loss coefficients should be fairly reliable within the range of flow divisions which was used in the experiments. The coefficient values extrapolated outside of this range are less reliable because of inherent uncertainties. These extrapolated values were therefore underlined in Table 2 and caution or further verifications are recommended when using such data.

Comparisons of various junction configurations were made possible by calculating the mean combined head loss coefficient for each test series and such coefficients were used in the following discussion of effects of various junction parameters on the head losses.

Among the junction parameters studied, the relative lateral size expressed as D_3/D_1 ($=D_3/D_2$ because the main and outlet pipe

diameters were identical) had the greatest influence on junction head losses. In this notation, D is the pipe diameter and indices 1, 2 and 3 refer to the outlet, main and lateral pipes, respectively. The lowest losses were found for $D_3/D_1 = 1.0$ (in other words, $D_1 = D_2 = D_3$). In this case, the mean combined head loss coefficient varied from 0.305 to 0.719. For $D_3/D_1 = 0.7$, the mean head loss coefficient varied from 0.678 to 1.143. For $D_3/D_1 = 0.45$, the range of mean combined head loss coefficients was from 1.28 to 2.019 and, finally, for $D_3/D_1 = 0.25$, the range was from 4.713 to 5.902.

The lateral size affects the momentum of the lateral flow. For a particular discharge, the lateral flow momentum will increase proportionately with $(1/D_3)^2$. Since most of the lateral flow momentum is lost at the junction (particularly for $\theta = 90^\circ$), the configurations with small laterals and the resulting high lateral flow momentum yield the highest head losses.

The effects of the remaining junction parameters, such as the benching type, manhole base shape and lateral angle were rather minor. The benching had some effect on the losses for $D_3/D_1 = 1.0$ and 0.7, and the lateral angle $\theta = 90^\circ$. The benchings providing better flow guidance, such as those described as moulds 2A and 2B, produced somewhat lower losses.

The head loss coefficients K_{12} and K_{13} varied with the relative discharges ψ_{12} and ψ_{13} (see Fig. 5). The variations in K_{12} are moderate and this coefficient seems to increase slightly with the increasing relative discharge. The maximum values of $K_{12} = 1.0$ are obtained in the range of ψ_{12} from 0.5 to 1.0. For the lateral pipe, the head loss coefficient K_{13} varies sharply with ψ_{13} and the maximum values of about 16.0 are found for $\psi_{13} = 1.0$.

The combined head loss coefficients K_c obtained in this study are compared with those reported by others in Table 3. Such comparisons for similar junctions were made for a selected typical value of $Q_3/Q_1 = 0.6$. A fair agreement among the results from various studies is obvious from Table 3.

6.0 SUMMARY AND CONCLUSIONS

Extensive tests of 40 different configurations of junction manholes with the main pipe and a lateral indicate the following findings:

- (1) Head losses at junctions of the main and lateral pipes are affected by both the junction geometry and the relative lateral discharge ψ_{13} ($= Q_{\text{lateral}}/Q_{\text{outlet}} = 1 - \psi_{23} = 1 - Q_{\text{main}}/Q_{\text{outlet}}$).
- (2) Among the junction geometry parameters, the relative lateral size ($D_{\text{lateral}}/D_{\text{outlet}} = D_3/D_1$) had the strongest influence on the mean combined head loss coefficient of a particular junction configuration. The smaller the ratio D_3/D_1 , the larger the junction head losses. The effects of the remaining parameters, such as the junction benching, lateral angle and the manhole base shape on the mean combined head loss coefficient were relatively minor.
- (3) Large differences between head loss coefficients for the main and lateral pipes were observed. Although both coefficients generally increased with the increasing relative discharges ψ_{12} and ψ_{13} , the increases in the lateral head loss coefficient were much larger. For very low relative discharges, energy gains rather than losses were observed under some circumstances.
- (4) For practical applications of the results presented above, it is recommended to reduce junction head losses by designing the junction of the main and lateral pipes with the following features:
 - (a) $D_3 = D_2 = D_1$.
 - (b) Ideally, the discharges should be in the range $0.7 \leq \psi_{12} < 1.0$ and $0 < \psi_{13} \leq 0.3$.
 - (c) Both square and round base manholes are acceptable.

- (d) Because the effects of the lateral angles θ on the mean combined head losses were minor, any of the angles studied (45° , 60° and 90°) is acceptable.
- (e) The junction benching should be used, particularly for large lateral angles (90°). The benching described as mould 2B and its modified version with benches at the pipe crown level are recommended.

7.0 REFERENCES

1. Jamison, D.K. and J.R. Villemonte, "Junction Losses in Laminar and Transitional Flows", Journal of the Hydraulics Division, ASCE, vol. 97, no. HY 7, Proc. Paper 8258, July 1971, pp. 1045-1063.
2. Jensens, M., "Hydraulic Energy Relations for Combined Flow and Their Application to the 90° Junction". Series Paper No. 11, Institute for Town and Country Planning, The Royal Veterinary and Agricultural University, Copenhagen, Dec. 1981.
3. Ito H. and K. Imai, "Energy Loss at 90° Pipe Junctions", Journal of the Hydraulics Division, ASCE, vol. 99, no. HY 9, 1973 pp. 1353-1368.
4. Marsalek, J., "Energy Losses at Straight-Flow-Through Sewer Junctions", Research Report No. 111, Training and Technology Transfer Div., EPS, Environment Canada, Ottawa, Ontario, K1A 1C8, 1981.
5. McNown, J.S., "Mechanics of Manifold Flow", Transactions ASCE, vol. 119, 1954, pp. 1103-118,
6. Miller, D.S., "Internal Flow: A Guide to Losses in Pipe and Duct Systems", The British Hydromechanics Research Association, Cranfield, Bedford, England, 1971.
7. Ruus, E., "Head Losses in Wyes and Manifolds", Journal of the Hydraulics Division, Proceedings of the American Society of Civil Engineers, vol. 96, no. HY3, March 1970, pp. 593-607.
8. Sangster, W.M., H.W. Wood, E.T. Smerdon, and H.G. Bossy, "Pressure Changes at Open Junctions in Conduits", Journal of the Hydraulics Division, Proc. of the American Society of Civil Engineers, vol. 85, HY6, 1959, pp. 13-41.
9. Townsend, K.D. and J.R. Prins, "Performance of Model Storm Sewer Junctions", Technical Notes, Journal of the Hydraulics Division, Proceedings of the American Society of Civil Engineers, vol. 104, no. HY1, January 1978, pp. 99-104.

12. Sevuk, A. Suha, B.C. Yen, "Sewer Network Routing by Dynamic Wave Characteristics", Journal of the Hydraulics Division, Proc. of the American Society of Civil Engineers, vol. 108, no HY3, March 1982, pp. 379-398.
13. Townsend, K.D. and J.R. Prins, "Performance of Model Storm Sewer Junctions", Technical Notes, Journal of the Hydraulics Division, Proceedings of the American Society of Civil Engineers, vol. 104, no. HY1, January 1978, pp. 99-104.

TABLES

TABLE 1. Coefficients of Regression Quadratic Polynomials

Test Series	$K_{12} = a + b\psi_{12} + c\psi_2^2$				$K_{13} = d + e\psi_{13} + f\psi_{13}^2$			
	a	b	c	R ²	d	e	f	R ²
1	.115	1.514	-.870	.900	-.312	.643	15.461	1.00
2	.251	1.427	-.616	.962	-.182	.415	15.743	1.00
3	.317	.661	.105	.988	-.099	.039	16.19	1.00
4	.140	2.097	-1.433	.819	-.720	2.690	13.700	1.00
5	.200	1.568	-.909	.991	-.160	.037	15.880	1.00
6	.037	1.401	-.762	.969	-.283	.104	16.948	1.00
7	-.010	2.276	-1.510	.866	-.308	1.367	3.878	1.00
8	-.263	3.044	-1.973	.991	-.213	1.052	4.165	.999
9	.307	.684	-.221	.913	-.254	1.222	3.996	.998
10	-.062	2.236	-1.354	.972	-.122	.444	5.148	.999
11	-.106	3.088	-2.384	.992	-.493	2.457	2.811	.999
12	.245	2.524	-2.050	.935	-.295	1.529	3.895	.999
13	-.480	3.719	-2.496	.979	-.351	1.897	3.388	.999
14	-.047	1.999	-1.139	.934	-.154	.162	5.089	.998
15	.414	1.861	-1.683	.888	-.400	1.810	16.410	1.00
16	.721	1.227	-1.099	.847	-.256	1.070	16.160	1.00
17	.617	1.448	-1.501	.948	.164	-.253	14.328	.999
18	-.388	2.562	-1.299	.988	-.546	2.273	2.831	.999
19	-.047	1.857	-1.063	.975	-.610	1.766	3.932	.988
20	-3.171	10.115	-6.281	.948	-.821	-4.833	-1.010	.953
21	.131	1.331	-.550	.940	-.723	3.759	1.464	.999
22	-.450	3.969	-2.922	.916	-.680	4.506	-2.945	.985
23	-.017	2.540	-1.746	.658	-.268	1.850	.631	.993

TABLE 1. (continued)

Test No.	$K_{12} = a + b\psi_{12} + C\psi_{12}^2$				$K_{13} = d + e\psi_{13} + f\psi_{13}^2$			
	a	b	c	R ²	d	e	f	R ²
24	-.021	2.727	-2.065	.768	-.326	2.200	.216	.998
25	-.184	2.788	-1.823	.942	-.2289	1.216	1.263	.997
26	-.793	5.526	-4.045	.680	-.492	2.858	-.284	.998
27	-.059	2.356	-1.541	.969	-.196	.921	1.819	.994
28	-.156	3.053	-2.305	.862	-.324	2.122	.342	.999
29	-.002	2.176	-1.389	.958	-.234	1.342	1.098	.955
30	-1.161	6.137	-4.526	.933	-.578	2.893	-.553	.995
31	-.376	3.432	-2.434	.943	-.649	2.769	-.275	.996
32	-.534	4.201	-3.287	.926	-.595	2.790	-.317	.999
33	-1.457	6.009	-4.162	.965	-.525	2.205	-.317	.994
34	-1.384	6.485	-4.643	.945	-.715	3.584	-2.318	.987
35	-.353	3.868	-2.979	.891	-.740	3.124	-1.380	.995
36	-.648	3.902	-2.605	.980	-.884	4.747	-4.396	.998
37	-2.755	9.336	-6.135	.914	-.690	3.019	-1.898	.984
38*	-.387	4.167	-3.190	.949	-.578	3.088	2.178	.999
39*	-.529	3.825	-2.943	.833	-.600	2.358	.060	.998
40*	-1.603	6.749	-4.730	.941	-.644	2.409	-.553	.976

* Round Base Manhole

TABLE 2. Combined Head Loss Coefficients for Various Lateral Inflows

Test Series	$K_C = K_{12}\psi_{12} + K_{13}\psi_{13} \quad (\psi_{12} + \psi_{13} = 1.0)$											Statistical Measures			Junction Configurations			
	$\psi_{13} =$.1	.2	.3	.4	.5	.6	.7	.8	.9	1.0	R_C	σ	σ/R	A_3/A_1	A_2/A_1	θ	M
1		.686	.703	.906	1.394	2.265	3.616	5.547	8.155	<u>11.547*</u>	<u>15.792*</u>	5.060	5.224	1.033	.250	1.000	45°	0
2		.934	.905	1.071	1.532	2.386	3.730	5.663	8.283	<u>11.6887</u>	<u>15.976</u>	5.217	5.219	1.00	.250	1.000	45°	1
3		.904	.842	.993	1.454	2.321	3.691	5.660	8.326	<u>11.783</u>	<u>16.130</u>	5.210	5.297	1.017	.250	1.000	45°	4
4		.749	.794	1.030	1.549	2.440	3.795	5.705	8.260	<u>11.552</u>	<u>15.670</u>	5.154	4.659	.789	.250	1.000	60°	0
5		.788	.795	.981	1.446	2.293	3.620	5.530	8.122	<u>11.497</u>	<u>15.757</u>	5.083	5.178	1.019	.250	1.000	60°	1
6		.602	.619	.833	1.350	2.277	3.719	5.783	8.575	<u>12.202</u>	<u>16.769</u>	5.273	5.591	1.060	.250	1.000	60°	4
7		.721	.700	.726	.831	1.048	1.408	1.945	<u>2.691</u>	<u>3.677</u>	<u>4.937</u>	1.868	1.465	.784	.445	1.000	45°	0
8		.784	.760	.774	.862	1.060	1.406	1.937	<u>2.689</u>	<u>3.699</u>	<u>5.004</u>	1.897	1.466	.772	.445	1.000	45°	1
9		.660	.600	.615	.730	.971	1.362	1.929	<u>2.696</u>	<u>3.690</u>	<u>4.934</u>	1.819	1.505	.827	.445	1.000	45°	3
10		.766	.723	.730	.827	1.052	1.445	2.044	<u>2.889</u>	<u>4.018</u>	<u>5.470</u>	1.996	1.642	.822	.445	1.000	45°	4
11		.646	.693	.770	.909	1.140	1.495	2.005	<u>2.701</u>	<u>3.614</u>	<u>4.775</u>	1.875	1.409	.752	.445	1.000	60°	0
12		.760	.795	.859	.989	1.219	1.585	2.124	2.870	<u>3.860</u>	<u>5.129</u>	2.019	1.495	.740	.445	1.000	60°	1
13		.748	.751	.787	.892	1.100	1.447	1.969	2.701	<u>3.677</u>	<u>4.934</u>	1.901	1.444	.760	.445	1.000	60°	3
14		.738	.675	.662	.735	.933	1.293	1.852	<u>2.647</u>	<u>3.717</u>	<u>5.097</u>	1.835	1.531	.834	.445	1.000	60°	4

* Underlined values were extrapolated and may contain significant uncertainties

TABLE 2. Combined Head Loss Coefficients for Various Lateral Inflows (continued)

Test Series	$K_C = K_{12}\psi_{12} + K_{13}\psi_{13} \quad (\psi_{12} + \psi_{13} = 1.0)$											Statistical Measures			Junction Configurations		
	$\psi_{13} =$.1	.2	.3	.4	.5	.6	.7	.8	.9	1.0	R_C	σ	σ/R_C	A_3/A_1	A_2/A_1	θ
15		.648	.784	1.110	1.735	2.766	4.312	6.482	9.384	13.127	17.820	5.817	5.898	1.014	.250	1.000	90°
16		.843	.920	1.185	1.740	2.689	4.137	6.185	8.938	12.500	16.974	5.611	5.558	.990	.250	1.000	90°
17		.662	.784	1.040	1.504	2.293	3.485	5.180	7.475	10.462	14.039	4.713	4.650	.986	.250	1.000	90°
18		.750	.669	.665	.735	.933	1.274	1.782	2.482	3.399	4.558	1.724	1.351	.784	.445	1.000	90°
19		.648	.587	.595	.701	.936	1.329	1.911*	2.712*	3.761*	5.088*	1.827	1.561	.854	.445	1.000	90°
20		.726	.742	.744	.762	.830	.977	1.237	1.639	2.217	3.002	1.288	4.854	1.094	.445	1.000	90°
21		.762	.693	.716	.845	1.091	1.466	1.982	2.652	3.487	4.500	1.819	1.329	.731	.445	1.000	90°
22		.654	.705	.745	.788	.819	.844	.862	.872	.875	.871	.804	.078	.097	.694	1.000	45°
23		.762	.743	.737	.756	.816	.929	1.112	1.377	1.739	2.213	1.118	.508	.454	.694	1.000	45°
24		.674	.696	.719	.759	.827	.939	1.107	1.346	1.669	2.090	1.083	.479	.443	.694	1.000	45°
25		.754	.717	.687	.684	.725	.830	1.016	1.303	1.708	2.251	1.067	.533	.499	.694	1.000	45°
26		.793	.845	.867	.882	.912	.980	1.109	1.320	1.637	2.082	1.143	.421	.368	.694	1.000	60°
27		.723	.684	.658	.665	.727	.862	1.091	1.434	1.912	2.544	1.130	.645	.571	.694	1.000	60°

* Underlined values were extrapolated and may contain appreciable uncertainties

TABLE 2. Combined Head Loss Coefficients for Various Lateral Inflows (continued)

Test Series	$K_C = K_{12}\psi_{12} + K_{13}\psi_{13} \ (\psi_{12} + \psi_{13} = 1.0)$											Statistical Measures			Junction Configurations			
	$\psi_{13} =$.1	.2	.3	.4	.5	.6	.7	.8	.9	1.0	R_C	σ	σ/R_C	A_3/A_1	A_2/A_1	θ	M
28		.641	.672	.699	.739	.808	.922	<u>1.096</u>	<u>1.346</u>	<u>1.689</u>	<u>2.140</u>	1.075	.504	.469	.694	1.000	60°	3
29		.739	.696	.669	.674	.725	.838	<u>1.028</u>	<u>1.309</u>	<u>1.697</u>	<u>2.206</u>	1.058	.525	.496	.694	1.000	60°	4
30		.597	.677	.714	.731	.753	<u>.803</u>	<u>.905</u>	<u>1.083</u>	<u>1.361</u>	<u>1.762</u>	.939	.367	.390	.694	1.000	90°	0
31		.630	.628	.631	.650	.699	.791	<u>.939</u>	<u>1.155</u>	<u>1.453</u>	<u>1.845</u>	.942	.419	.445	.694	1.000	90°	1
32		.494	.569	.621	.670	.733	.827	<u>.971</u>	<u>1.182</u>	<u>1.479</u>	<u>1.878</u>	.942	.447	.474	.694	1.00	90°	2A
33		.491	.530	.529	.513	.503	<u>.523</u>	<u>.596</u>	<u>.745</u>	<u>.993</u>	<u>1.363</u>	.678	.287	.423	.694	1.000	90°	2B
34		.585	.648	.662	.640	.598	<u>.547</u>	<u>.504</u>	<u>.480</u>	<u>.492</u>	<u>.551</u>	.571	.067	.117	1.000	1.000	90°	0
35		.600	.634	.648	.653	.657	<u>.670</u>	<u>.701</u>	<u>.761</u>	<u>.859</u>	<u>1.004</u>	.719	.125	.174	1.000	1.000	90°	1
36		.633	.623	.608	.578	<u>.521*</u>	<u>.427</u>	<u>.286</u>	<u>.086</u>	<u>-.184</u>	<u>-.533</u>	.305	.398	1.307	1.000	1.000	90°	2A
37		.570	.597	.555	.468	<u>.362</u>	<u>.262</u>	<u>.193</u>	<u>.182</u>	<u>.252</u>	<u>.431</u>	.387	.159	.411	1.000	1.000	90°	2B
38		.677	.749	.840	.981	1.204	1.541	<u>2.026</u>	<u>2.689</u>	<u>3.563</u>	<u>4.680</u>	1.895	1.355	.715	.445	1.000	90°	2A
39		.440	.493	.528	.565	.621	.714	<u>.862</u>	<u>1.083</u>	<u>1.396</u>	<u>1.818</u>	.852	.452	.531	.694	1.000	90°	2A
40		.535	.578	.571	.539	<u>.506</u>	<u>.497</u>	<u>.539</u>	<u>.655</u>	<u>.871</u>	<u>1.212</u>	.650	.226	.347	1.000	1.000	90°	2A

* Underlined values are extrapolated and may contain appreciable uncertainties

TABLE 3. Comparison of Head Loss Coefficients from Various Sources

	Source	Junction Base	Junction Benching	Lateral Pipe Angle	D_1/D_3	Q_3/Q_1	b^*/D_1	Flow Type			K_c
								Combined or Divided	Free Surface	Pressurized Flow	
1	Sangster et al (11)	Square Round	None None	90° 90°	1.00 1.27	.6 .6	1.87 2.08	Combined Combined		yes yes	1.040 .708
2	Townsend & Prins (13)	Rectangular	Drop invert	45°	1.57	.6	2.55	Combined	Yes		1.058
3	Present Study	Square Round	Drop invert ditto ditto M=2A	45° 60° 90° 90°	1.20 1.20 1.20 1.20	.6 .6 .6 .6	2.26 2.26 2.26 2.23	Combined Combined Combined Combined		Yes Yes Yes	.844 .980 .803 .714

* b is the width of manhole junction

FIGURES

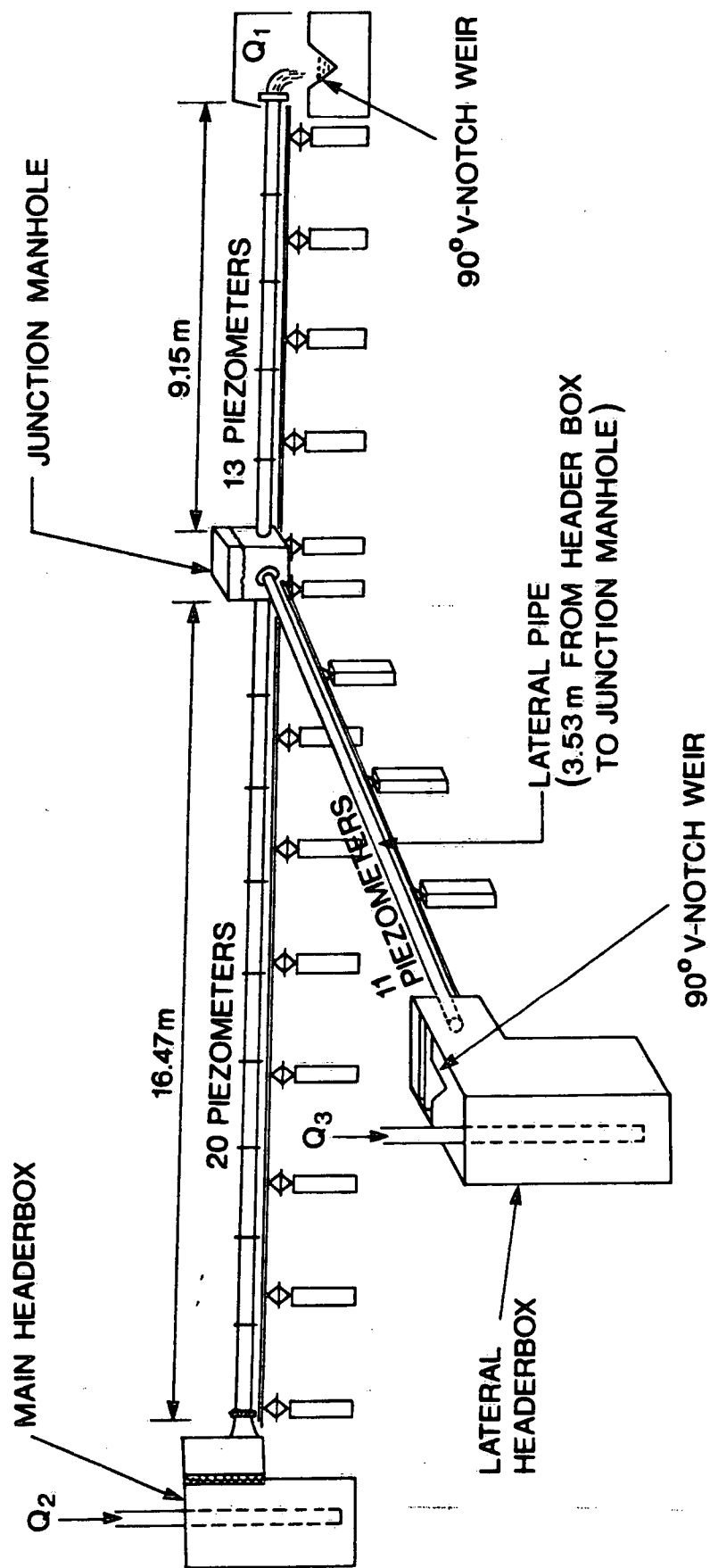


FIGURE 1.
GENERAL LAYOUT OF EXPERIMENTAL APPARATUS (not drawn to scale)

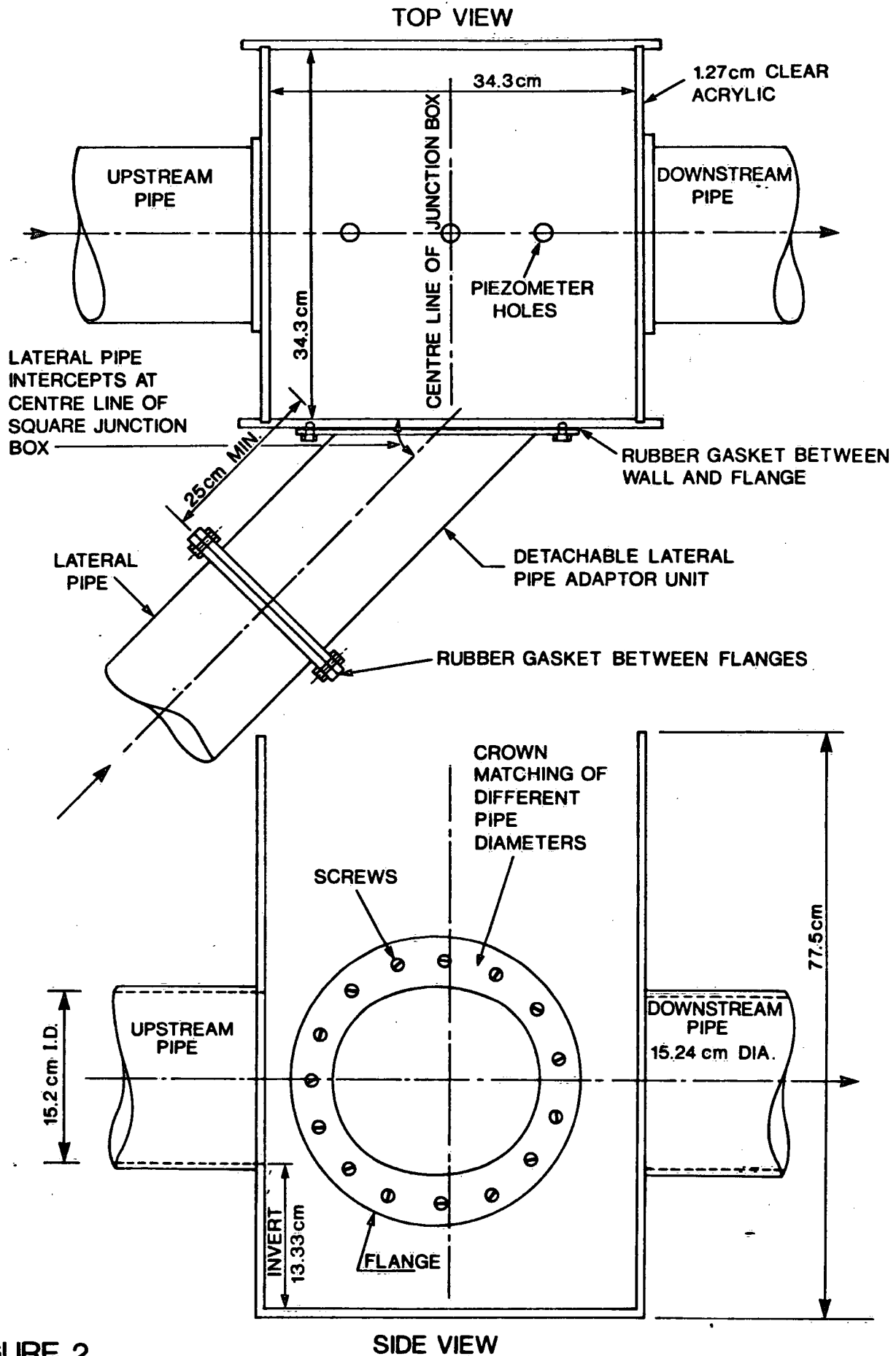


FIGURE 2.

JUNCTION BOX WITH A LATERAL PIPE INLET ASSEMBLY (not drawn to scale)

LATERAL PIPE SIZE (mm)	JUNCTION TYPE	ISOMETRIC VIEW	PLAN VIEW	SIDE VIEW
76 (3") 102 (4") 127 (5") 152 (6")	SQUARE JUNCTION	NO MOULD 	$\theta = 90^\circ$ $\theta = 60^\circ$ $\theta = 45^\circ$ DEFLECTOR 	
		MOULD #1 		
76 (3") 102 (4") 127 (5") 152 (6")	SQUARE JUNCTION	MOULD #2A 	$\theta = 90^\circ$ 	
		MOULD #2B 		
76 (3") 102 (4") 127 (5")	SQUARE JUNCTION	MOULD #1 	$\theta = 45^\circ, 60^\circ$ DEFLECTOR 	
		MOULD #4 45° DEFLECTOR 		
76 (3") 102 (4") 127 (5")	SQUARE JUNCTION	MOULD #3 	$\theta = 45^\circ, 60^\circ$ 	
		MOULD #3 		
102 (4") 127 (5") 152 (6")	CIRCULAR JUNCTION	MOULD #2A 	$\theta = 90^\circ$ 	
			METAL SHEET LINER 	

FIGURE 3 JUNCTION MANHOLES TESTED

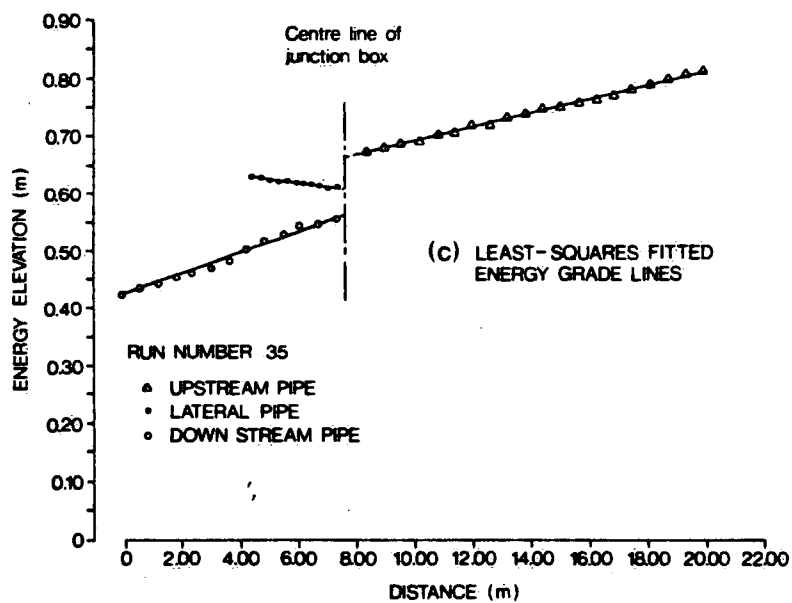
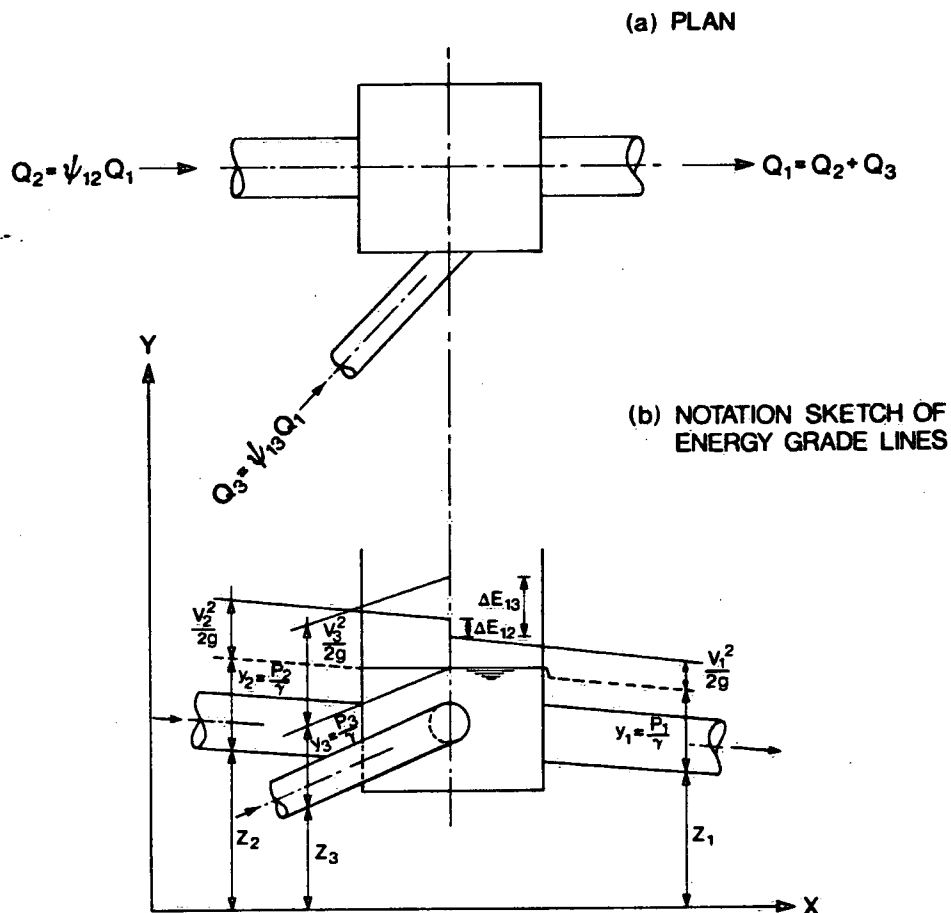


FIGURE 4. NOTATION SKETCH

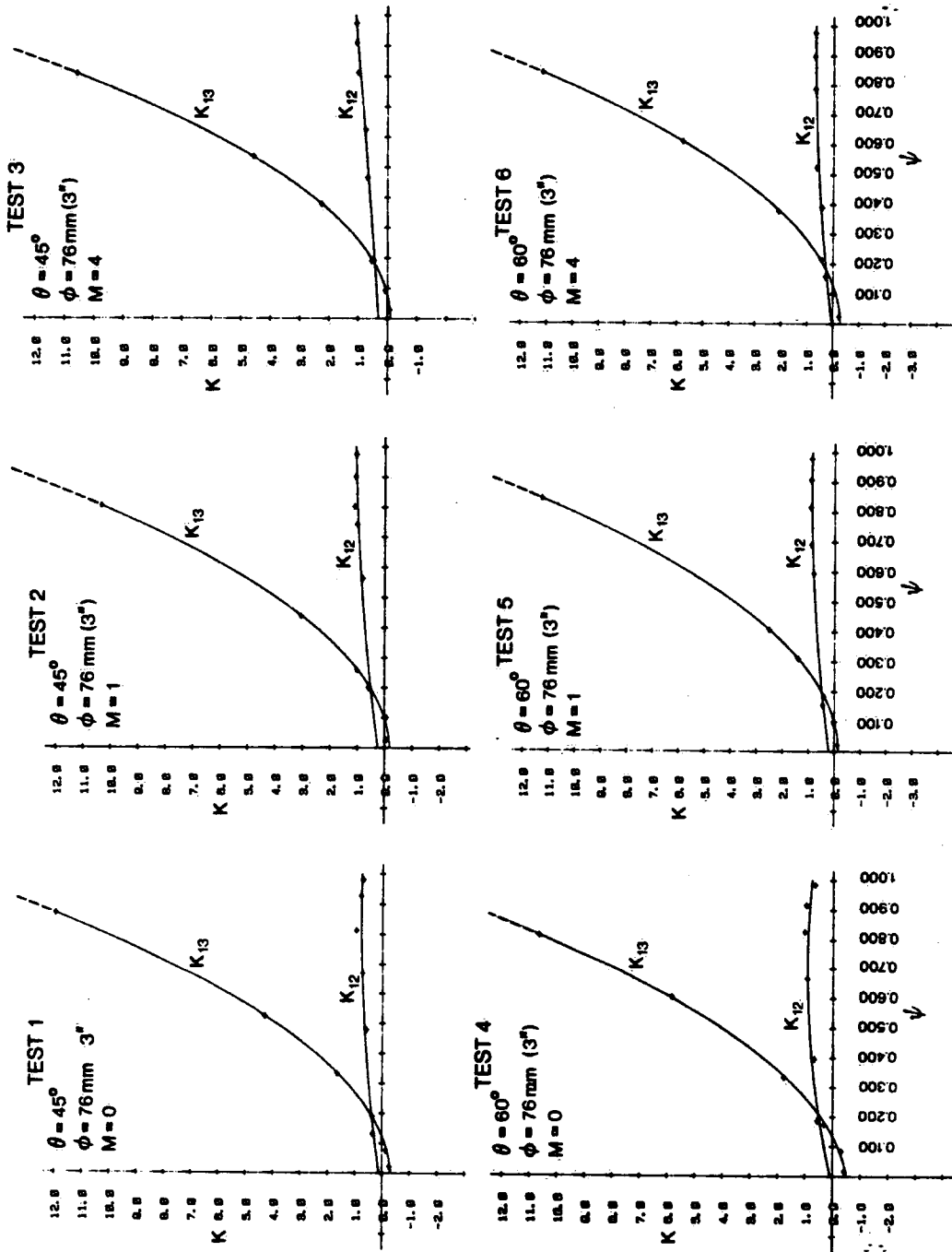


FIGURE 5(a). HEAD LOSS COEFFICIENT VS THE RELATIVE LATERAL INFLOW.

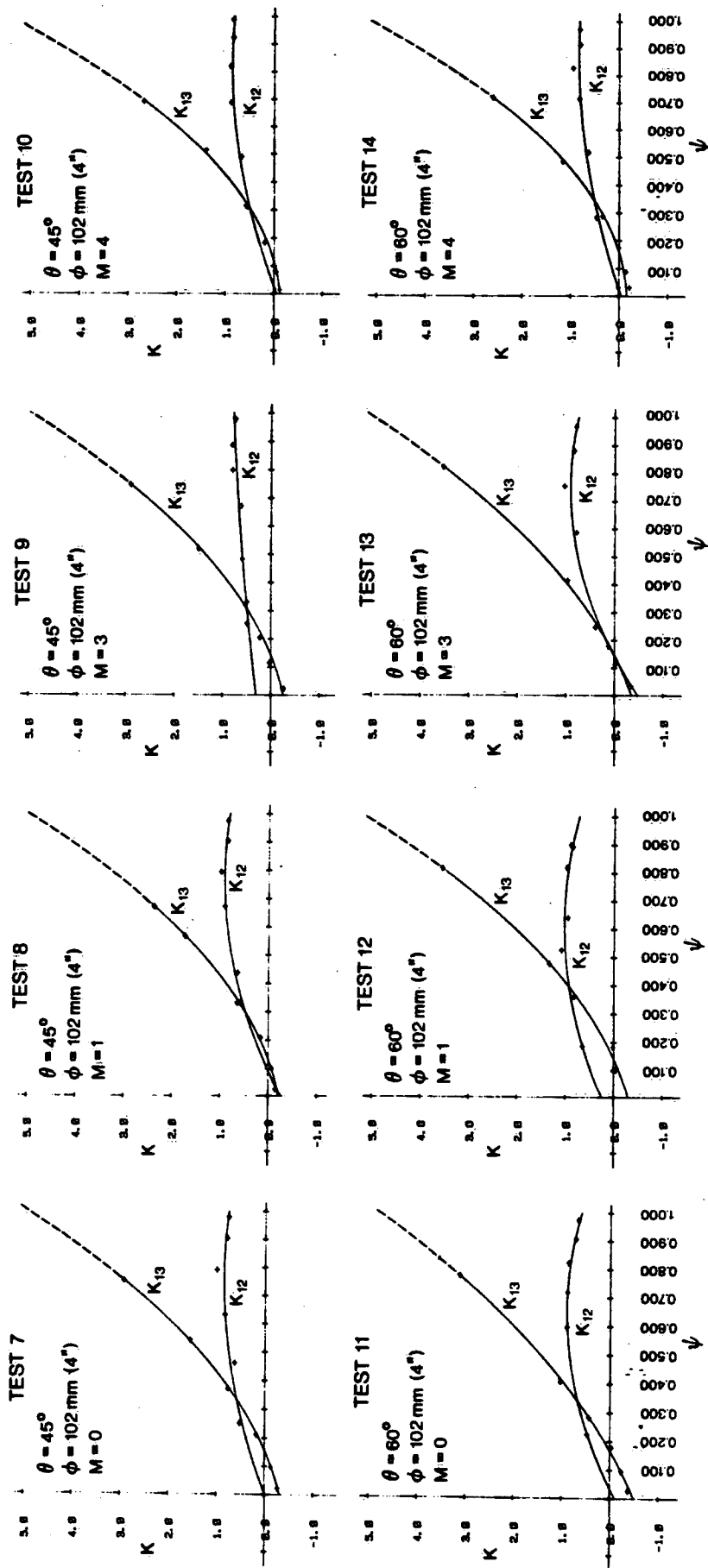


FIGURE 5(b). HEAD LOSS COEFFICIENT VS THE RELATIVE LATERAL INFLOW.

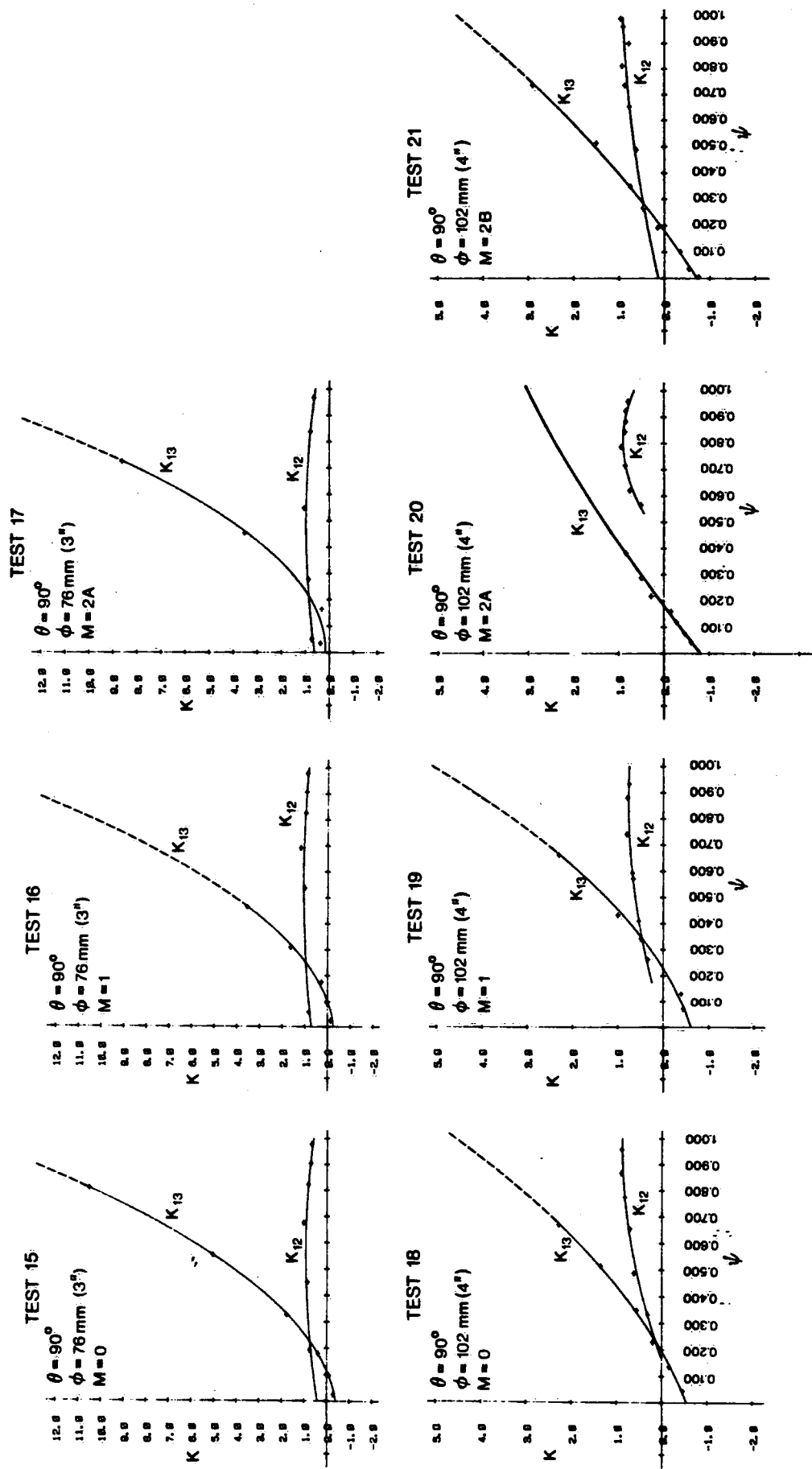


FIGURE 5(c). HEAD LOSS COEFFICIENT VS THE RELATIVE LATERAL INFLOW.

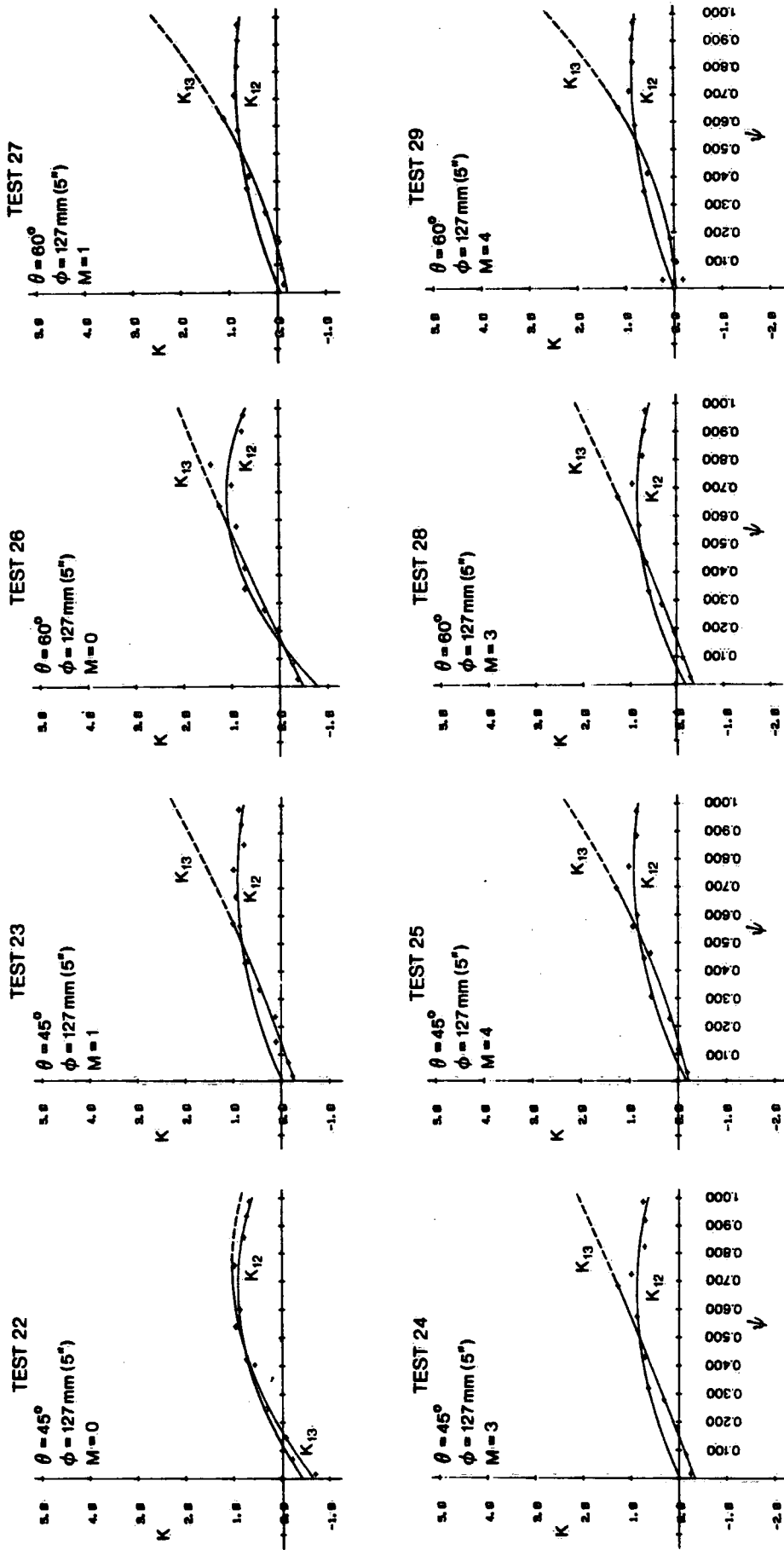


FIGURE 5(d). HEAD LOSS COEFFICIENT VS THE RELATIVE LATERAL INFLOW.

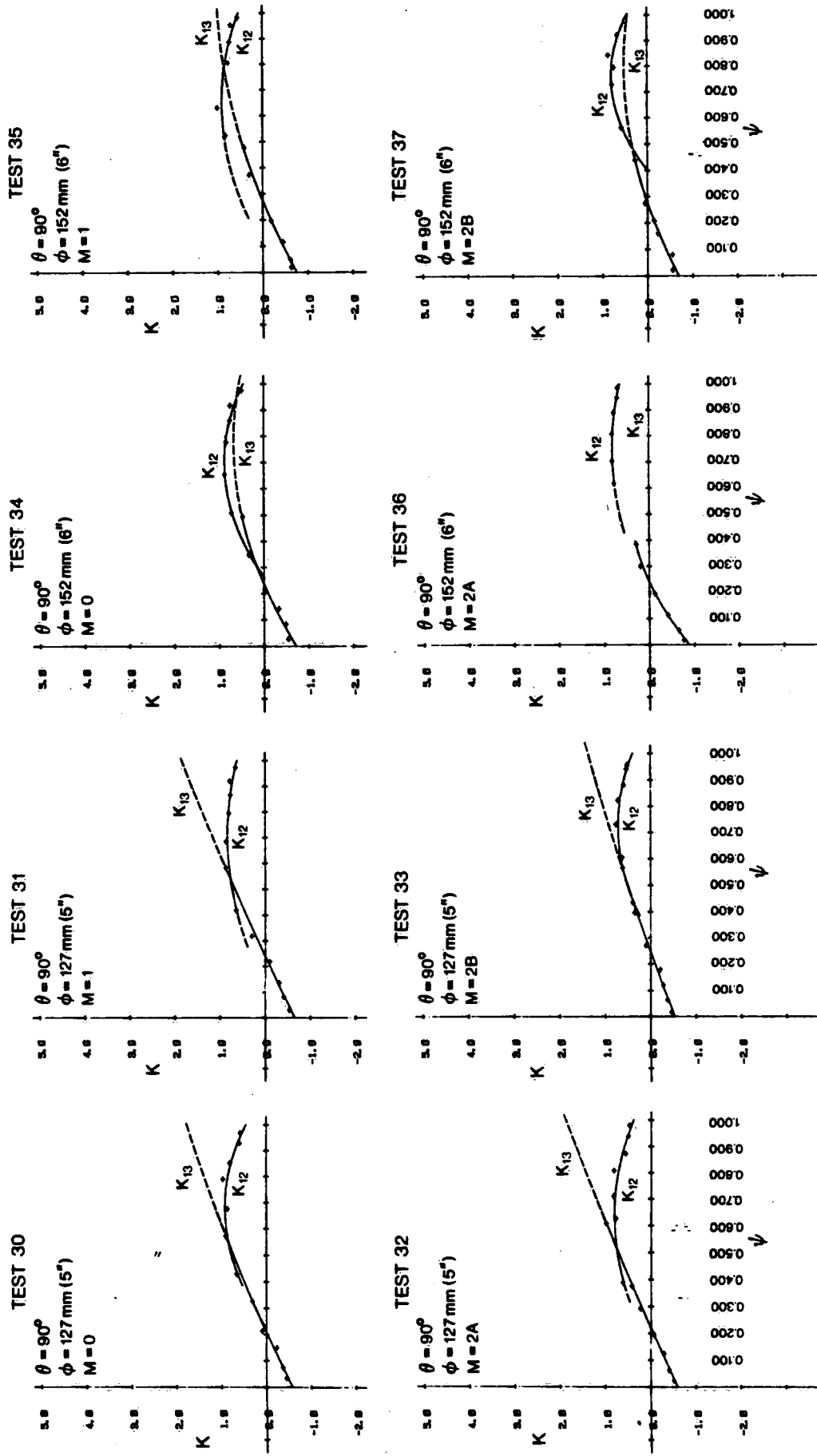


FIGURE 5(e). HEAD LOSS COEFFICIENT VS THE RELATIVE LATERAL INFLOW.

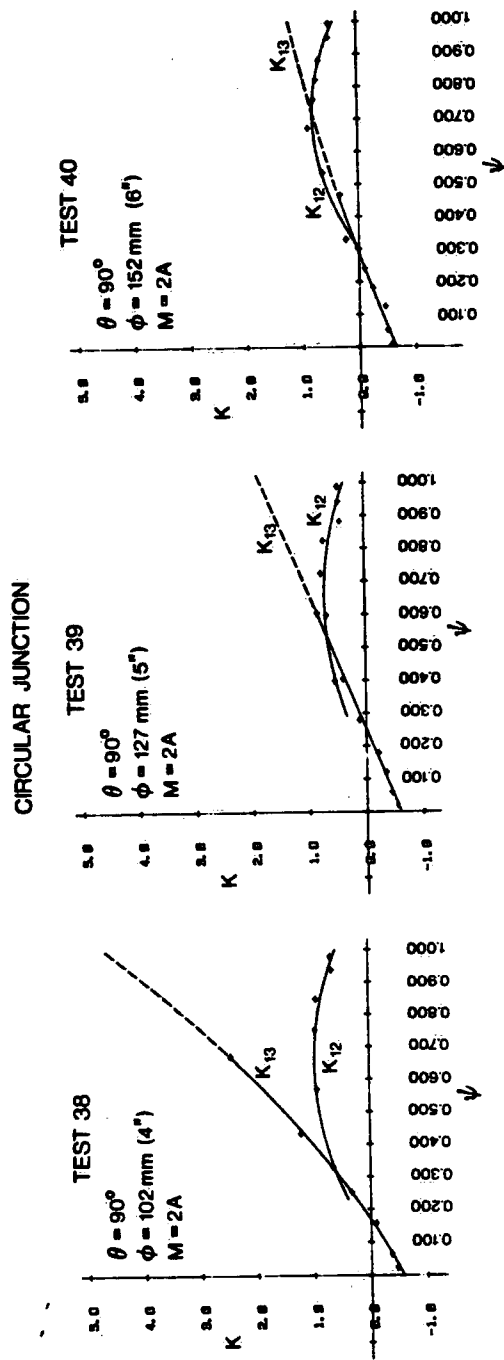


FIGURE 5(f). HEAD LOSS COEFFICIENT VS THE RELATIVE LATERAL INFLOW.